

Quark-meson coupling model for antikaon condensation in neutron star matter with strong magnetic fields

P. Yue and H. Shen*

Department of Physics, Nankai University, Tianjin 300071, People's Republic of China

(Received 15 June 2007; revised manuscript received 8 November 2007; published 25 April 2008)

We study the effects of strong magnetic fields on antikaon condensation in neutron star matter using the quark-meson coupling (QMC) model. The QMC model describes a nuclear many-body system as nonoverlapping MIT bags in which quarks interact through the self-consistent exchange of scalar and vector mesons in the mean-field approximation. It is found that the presence of strong magnetic fields alters the threshold density of antikaon condensation significantly. The onset of K^- condensation stronger depends on the magnetic field strength, and it even shifts beyond the threshold of \bar{K}^0 condensation for sufficiently strong magnetic fields. In the presence of strong magnetic fields, the equation of state (EOS) becomes stiffer in comparison with the field-free case. The softening of the EOS by antikaon condensation also depends on the magnetic field strength, and it becomes less pronounced with increasing magnetic field strength. The results of the QMC model are compared with those obtained in a relativistic mean-field (RMF) model, and we find there are quantitative differences between the results of the QMC and RMF models.

DOI: [10.1103/PhysRevC.77.045804](https://doi.org/10.1103/PhysRevC.77.045804)

PACS number(s): 26.60.-c, 24.10.Jv, 24.85.+p, 95.30.Cq

I. INTRODUCTION

The study of dense stellar matter in the presence of strong magnetic fields is of great interest in nuclear astrophysics. Observations of ordinary radio pulsars indicate that they possess surface magnetic fields of the order of 10^{12} G [1]. Recent surveys of soft-gamma repeaters (SGRs) and anomalous X-ray pulsars (AXPs) imply that the surface magnetic field of young neutron stars could be of order 10^{14} – 10^{15} G [2]. The magnetic field strength may vary significantly from the surface to the center in neutron stars. So far, there is no direct observational evidence for the internal magnetic fields of the star, while it may reach 10^{18} G, as estimated in some theoretical works [3–5]. Motivated by a possible existence of strong magnetic fields in neutron stars, theoretical studies on the effects of extremely large fields on dense matter have been carried out by many authors [1,3,5–8], and the inclusion of hyperons and boson condensation has also been investigated [9–11]. There have been some works that investigate the effects of strong magnetic fields on neutron star properties [4,5]. In Ref. [4], the authors studied static neutron stars with poloidal magnetic fields and a simple class of electric current distributions, and they found that the maximum mass among these static configurations with magnetic fields is noticeably larger than the maximum mass attainable with uniform rotation and no magnetic field. In Ref. [5], the authors assumed the magnetic field varies from the surface to the center in neutron stars, and they found that the maximum mass of neutron stars could substantially increase if the strongest possible magnetic fields existed in the center of neutron stars.

It is believed that the density in the interior of neutron stars is extremely high, and additional degrees of freedom such as hyperons, kaons, and even quarks may occur in the core of neutron stars [12–15]. Recently, much attention

has been paid to the kaon/antikaon condensations based on various models [16–22]. In general, the presence of antikaon condensation tends to soften the equation of state (EOS) at high density and lower the maximum mass of neutron stars. It is interesting to investigate the influence of strong magnetic fields on antikaon condensation. In Ref. [11], the condensation of negatively charged K^- under the influence of strong magnetic fields has been studied within a relativistic mean-field (RMF) model. It was found that the threshold of K^- condensation shifts to higher density in the presence of strong magnetic fields and the EOS becomes stiffer. These qualitative features are expected to persist in other models.

In this article, we study the effects of strong magnetic fields on the condensations of negatively charged K^- and neutral \bar{K}^0 in neutron star matter using the quark-meson coupling (QMC) model. The QMC model was originally proposed in the article by Guichon [23], in which the quark degrees of freedom are explicitly taken into account and a nuclear many-body system is described as a collection of nonoverlapping MIT bags interacting through the self-consistent exchange of meson mean fields. The QMC model has been extended and applied to various problems of nuclear matter and finite nuclei with reasonable success [24–27]. Furthermore, the model has also been used to investigate the properties of neutron stars with the inclusion of hyperons, quarks, and K^- condensation [14,15,22]. In the present work, both nucleons and antikaons are described as MIT bags that interact through the self-consistent exchange of isoscalar scalar and vector mesons (σ and ω) and isovector vector meson (ρ) in the mean-field approximation. These exchanged mesons couple directly to the confined quarks inside the bags. In contrast to the RMF model, the quark structure plays a crucial role in the QMC model, and the basic coupling constants are defined at the quark level. In Ref. [28], the in-medium kaon and antikaon properties have been studied in the QMC model. In Ref. [22], the consequences of including K^- condensation on the EOS of neutron star matter and related compact star properties have

*songtc@nankai.edu.cn

been investigated using the QMC model. Next, we examine the effects of strong magnetic fields on K^- and \bar{K}^0 condensations occurring in neutron star matter within the QMC model.

The aim of the present article is to investigate the influence of strong magnetic fields on antikaon condensation that may occur in the core of massive stars. For antikaon condensation in the field-free case, there have been many discussions in the literature after the paper by Kaplan and Nelson [29] who pointed out the possibility of the existence of K^- condensation in dense nuclear matter. In general, the chemical potential of antikaons in dense matter decreases with increasing density due to their interaction with nucleons. As a consequence, the ground state of hadronic matter at high density might contain antikaon condensation. The appearance of antikaon condensation can soften the EOS of neutron star matter and lower the maximum mass of neutron stars [16,22]. However, it is known that the surface magnetic field of young neutron stars can be of order 10^{14} – 10^{15} G [2], whereas the internal magnetic fields of the star may reach 10^{18} G, as estimated in some theoretical works [3–5]. The possible existence of strong magnetic fields in neutron stars motivates us to study the effects of extremely strong magnetic fields on dense matter. It has been found that the composition and the EOS of neutron star matter can be significantly affected by strong magnetic fields [3,7,8], while the maximum mass of neutron stars might substantially increase if the strongest possible magnetic fields existed in the center of neutron stars [4,5]. Because antikaon condensation can be important in the understanding of neutron stars, an investigation of the influence of strong magnetic fields on antikaon condensation would be of interest for the study of compact stars in astrophysics.

This article is arranged as follows. In Sec. II, we briefly describe the QMC model for neutron star matter with antikaon condensation in the presence of strong magnetic fields. In Sec. III, we show and discuss the numerical results in the QMC model and make a systematic comparison with the results of the RMF model. Section IV is devoted to a summary.

II. FORMALISM

We adopt the QMC model to describe neutron star matter with antikaon condensation in the presence of strong magnetic fields. In the QMC model, nucleons and antikaons are described as MIT bags that interact through the self-consistent exchange of isoscalar scalar and vector mesons (σ and ω) and isovector vector meson (ρ) in the mean-field approximation. To perform the calculation for neutron star matter in the presence of strong magnetic fields, we first study the properties of nucleons and antikaons under the influence of external meson and electromagnetic fields using the MIT bag model. These external fields are in principle functions of position in the bag, which may cause a deformation of the bag. For simplicity, we neglect the spatial variation of the fields over the small bag volume and take the values at the center of the bag as their average quantities [24]. We note that the spherical bag approximation may be violated in a superstrong magnetic field where the deformation of the bag can be significant.

For nucleons described as spherical MIT bags with external meson and electromagnetic fields, the up and down quarks

inside the bag satisfy the Dirac equation

$$\left[i\gamma_\mu \partial^\mu - (m_q + g_\sigma^q \sigma) - g_\omega^q \omega_\mu \gamma^\mu - g_\rho^q \tau_{3q} \rho_{3\mu} \gamma^\mu - \frac{e(1 + 3\tau_{3q})}{6} A_\mu \gamma^\mu \right] \psi_q = 0, \quad (1)$$

where g_σ^q , g_ω^q , and g_ρ^q are the quark-meson coupling constants and m_q is the current quark mass. τ_{3q} is the third component of the Pauli matrices. σ , ω_μ , $\rho_{3\mu}$, and A_μ are the values of the meson and electromagnetic fields at the center of the bag.

The normalized ground state for a quark in the bag is given by

$$\psi_q(\mathbf{r}, t) = \mathcal{N}_q e^{-i\epsilon_q t / R_N} \begin{bmatrix} j_0(x_q r / R_N) \\ i \beta_q \vec{\sigma} \cdot \hat{\mathbf{r}} j_1(x_q r / R_N) \end{bmatrix} \frac{\chi_q}{\sqrt{4\pi}}, \quad (2)$$

where

$$\beta_q = \sqrt{\frac{\Omega_q - R_N m_q^*}{\Omega_q + R_N m_q^*}}, \quad (3)$$

$$\mathcal{N}_q^{-2} = 2 R_N^3 j_0^2(x_q) [\Omega_q (\Omega_q - 1) + R_N m_q^* / 2] / x_q^2, \quad (4)$$

with $\Omega_q = \sqrt{x_q^2 + (R_N m_q^*)^2}$ and $m_q^* = m_q + g_\sigma^q \sigma$. R_N is the bag radius of the nucleon, and χ_q is the quark spinor. The boundary condition, $j_0(x_q) = \beta_q j_1(x_q)$, at the bag surface determines the eigenvalue x_q . The energy of a static nucleon bag consisting of three ground-state quarks is then given by

$$E_N^{\text{bag}} = 3 \frac{\Omega_q}{R_N} - \frac{Z_N}{R_N} + \frac{4}{3} \pi R_N^3 B_N, \quad (5)$$

where the parameter Z_N accounts for various corrections including zero-point motion and B_N is the bag constant. The effective nucleon mass is then taken to be

$$M_N^* = E_N^{\text{bag}}. \quad (6)$$

The bag radius R_N is determined by the equilibrium condition $\partial M_N^* / \partial R_N = 0$. In the present calculation, we take the current quark mass $m_q = 5.5$ MeV. The parameter $B_N^{1/4} = 210.854$ MeV and $Z_N = 4.00506$, as given in Ref. [15], are determined by reproducing the nucleon mass $M_N = 939$ MeV and the bag radius $R_N = 0.6$ fm in free space.

For antikaons, negatively charged K^- and neutral \bar{K}^0 , we assume that they are described as MIT bags in the same way as nucleons [22,28]. The exchanged σ , ω , and ρ mesons are assumed to couple exclusively to the up and down quarks (and antiquarks), not to the strange quark according to the Okubo-Zweig-Iizuka (OZI) rule [22]. Hence the antiquarks, \bar{u} in K^- and \bar{d} in \bar{K}^0 , and the s quarks satisfy the Dirac equations

$$\left[i\gamma_\mu \partial^\mu - (m_q + g_\sigma^q \sigma) + g_\omega^q \omega_\mu \gamma^\mu + g_\rho^q \tau_{3q} \rho_{3\mu} \gamma^\mu + \frac{e(1 + 3\tau_{3q})}{6} A_\mu \gamma^\mu \right] \psi_{\bar{q}} = 0, \quad (7)$$

and

$$\left(i\gamma_\mu \partial^\mu - m_s + \frac{e}{3} A_\mu \gamma^\mu \right) \psi_s = 0. \quad (8)$$

Similarly, the effective mass of antikaons and kaons is given by

$$m_K^* = \frac{\Omega_q + \Omega_s}{R_K} - \frac{Z_K}{R_K} + \frac{4}{3}\pi R_K^3 B_K, \quad (9)$$

where $\Omega_q = \sqrt{x_q^2 + (R_K m_q^*)^2}$ and $\Omega_s = \sqrt{x_s^2 + (R_K m_s)^2}$. We take the strange quark mass $m_s = 150$ MeV and the bag constant $B_K = B_N$. The parameters $Z_K = 3.362$ and $R_K = 0.457$ fm, as given in Ref. [22], are determined from the kaon mass and the stability condition in free space.

To describe neutron star matter with antikaon condensation in the presence of strong magnetic fields, we adopt the total Lagrangian density written at the hadron level as the sum of nucleonic, kaonic, and leptonic parts,

$$\mathcal{L} = \mathcal{L}_N + \mathcal{L}_K + \mathcal{L}_l, \quad (10)$$

where

$$\begin{aligned} \mathcal{L}_N = \sum_{b=n,p} \bar{\psi}_b \left[i\gamma_\mu \partial^\mu - q_b \gamma_\mu A^\mu - M_N^* - g_{\omega N} \gamma_\mu \omega^\mu \right. \\ \left. - g_{\rho N} \gamma_\mu \tau_{iN} \rho_i^\mu - \frac{1}{2} \kappa_b \sigma_{\mu\nu} F^{\mu\nu} \right] \psi_b \\ + \frac{1}{2} \partial_\mu \sigma \partial^\mu \sigma - \frac{1}{2} m_\sigma^2 \sigma^2 - \frac{1}{4} W_{\mu\nu} W^{\mu\nu} + \frac{1}{2} m_\omega^2 \omega_\mu \omega^\mu \\ - \frac{1}{4} R_{i\mu\nu} R_i^{\mu\nu} + \frac{1}{2} m_\rho^2 \rho_{i\mu} \rho_i^\mu - \frac{1}{4} F_{\mu\nu} F^{\mu\nu}, \end{aligned} \quad (11)$$

$$\mathcal{L}_K = D_\mu^* \bar{K} D^\mu K - m_K^{*2} \bar{K} K, \quad (12)$$

$$\mathcal{L}_l = \sum_{l=e,\mu} \bar{\psi}_l [i\gamma_\mu \partial^\mu - q_l \gamma_\mu A^\mu - m_l] \psi_l. \quad (13)$$

Here $A^\mu = (0, 0, Bx, 0)$ refers to a constant external magnetic field B along the z axis. The effective masses M_N^* and m_K^* in Eqs. (6) and (9) are obtained at the quark level. The covariant derivative is defined as $D_\mu = \partial_\mu + iq_K A_\mu + ig_{\omega K} \omega_\mu + ig_{\rho K} \tau_{iK} \rho_i^\mu$. The isospin doublet for kaons is denoted by $K \equiv (K^+, K^0)$ and that for antikaons by $\bar{K} \equiv (K^-, \bar{K}^0)$. We note that the electric charges of particles are $q_e = q_\mu = q_{K^-} = -e$, $q_n = q_{\bar{K}^0} = 0$, and $q_p = e$. The anomalous magnetic moments of nucleons are included with $\kappa_p = \mu_N(g_p/2 - 1) = 1.7928 \mu_N$ and $\kappa_n = \mu_N g_n/2 = -1.9130 \mu_N$, where μ_N is the nuclear magneton. In the QMC model, the coupling constants at the hadron level are related to the quark-meson coupling constants as $g_{\omega N} = 3g_\omega^q$, $g_{\omega K} = g_\omega^q$, and $g_{\rho N} = g_{\rho K} = g_\rho^q$ [22,28]. The quark-meson coupling constants $g_\sigma^q = 5.957$, $g_\omega^q = 2.994$, and $g_\rho^q = 4.325$ are determined by fitting the saturation properties of nuclear matter [15]. The meson masses $m_\sigma = 550$ MeV, $m_\omega = 783$ MeV, and $m_\rho = 770$ MeV are used in the present calculation.

In the mean-field approximation, the meson field equations in the presence of antikaon condensation and strong magnetic fields have the following forms:

$$\begin{aligned} m_\sigma^2 \sigma = -\frac{\partial M_N^*}{\partial \sigma} (\rho_s^p + \rho_s^n) \\ - \frac{\partial m_K^*}{\partial \sigma} \left(\frac{m_K^*}{\sqrt{m_K^{*2} + |q_{K^-}|B}} \rho_{K^-} + \rho_{\bar{K}^0} \right), \end{aligned} \quad (14)$$

$$m_\omega^2 \omega_0 = g_{\omega N} (\rho_v^p + \rho_v^n) - g_{\omega K} (\rho_{K^-} + \rho_{\bar{K}^0}), \quad (15)$$

$$m_\rho^2 \rho_{30} = g_{\rho N} (\rho_v^p - \rho_v^n) - g_{\rho K} (\rho_{K^-} - \rho_{\bar{K}^0}). \quad (16)$$

The Dirac equations for nucleons and leptons are given by

$$\begin{aligned} (i\gamma_\mu \partial^\mu - q_b \gamma_\mu A^\mu - M_N^* - g_{\omega N} \gamma^0 \omega_0 - g_{\rho N} \gamma^0 \tau_{3N} \rho_{30} \\ - \frac{1}{2} \kappa_b \sigma_{\mu\nu} F^{\mu\nu}) \psi_b = 0, \end{aligned} \quad (17)$$

$$(i\gamma_\mu \partial^\mu - q_l \gamma_\mu A^\mu - m_l) \psi_l = 0. \quad (18)$$

The energy spectra for protons, neutrons, and leptons (electrons and muons) are given by

$$\begin{aligned} E_{v,s}^p = \sqrt{k_z^2 + (\sqrt{M_N^{*2} + 2\nu q_p B} - s\kappa_p B)^2} \\ + g_{\omega N} \omega_0 + g_{\rho N} \rho_{30}, \end{aligned} \quad (19)$$

$$\begin{aligned} E_s^n = \sqrt{k_z^2 + (\sqrt{M_N^{*2} + k_x^2 + k_y^2} - s\kappa_n B)^2} \\ + g_{\omega N} \omega_0 - g_{\rho N} \rho_{30}, \end{aligned} \quad (20)$$

$$E_{v,s}^l = \sqrt{k_z^2 + m_l^2 + 2\nu |q_l| B}, \quad (21)$$

where $\nu = n + 1/2 - \text{sgn}(q_i) s/2 = 0, 1, 2, \dots$ enumerates the Landau levels of the fermion i with electric charge q_i ($i = p, e, \text{ or } \mu$). The quantum number s is $+1$ for spin up and -1 for spin down cases. The expressions of scalar and vector densities for protons and neutrons are given by

$$\begin{aligned} \rho_s^p = \frac{q_p B M_N^*}{2\pi^2} \sum_v \sum_s \frac{\sqrt{M_N^{*2} + 2\nu q_p B} - s\kappa_p B}{\sqrt{M_N^{*2} + 2\nu q_p B}} \\ \times \ln \left| \frac{k_{f,v,s}^p + E_f^p}{\sqrt{M_N^{*2} + 2\nu q_p B} - s\kappa_p B} \right|, \end{aligned} \quad (22)$$

$$\rho_v^p = \frac{q_p B}{2\pi^2} \sum_v \sum_s k_{f,v,s}^p, \quad (23)$$

$$\rho_s^n = \frac{M_N^*}{4\pi^2} \sum_s \left[k_{f,s}^n E_f^n - (M_N^* - s\kappa_n B)^2 \ln \left| \frac{k_{f,s}^n + E_f^n}{M_N^* - s\kappa_n B} \right| \right], \quad (24)$$

$$\begin{aligned} \rho_v^n = \frac{1}{2\pi^2} \sum_s \left\{ \frac{1}{3} k_{f,s}^{n3} - \frac{1}{2} s\kappa_n B [(M_N^* - s\kappa_n B) k_{f,s}^n \right. \\ \left. + E_f^n \left(\arcsin \frac{M_N^* - s\kappa_n B}{E_f^n} - \frac{\pi}{2} \right)] \right\}, \end{aligned} \quad (25)$$

where $k_{f,v,s}^p$ and $k_{f,s}^n$ are the Fermi momenta of protons and neutrons, which are related to the Fermi energies E_f^p and E_f^n as

$$E_f^{p2} = k_{f,v,s}^{p2} + \left(\sqrt{M_N^{*2} + 2\nu q_p B} - s\kappa_p B \right)^2, \quad (26)$$

$$E_f^{n2} = k_{f,s}^{n2} + (M_N^* - s\kappa_n B)^2. \quad (27)$$

The chemical potentials of nucleons and leptons are given by

$$\mu_p = E_f^p + g_{\omega N} \omega_0 + g_{\rho N} \rho_{30}, \quad (28)$$

$$\mu_n = E_f^n + g_{\omega N} \omega_0 - g_{\rho N} \rho_{30}, \quad (29)$$

$$\mu_l = E_f^l = \sqrt{k_{f,v,s}^2 + m_l^2} + 2\nu |q_l| B. \quad (30)$$

The equation of motion for antikaons $\bar{K} \equiv (K^-, \bar{K}^0)$ in neutron star matter with magnetic fields can be explicitly written as

$$(\partial_\mu - iq_{\bar{K}} A_\mu - ig_{\omega K} \omega_0 - ig_{\rho K} \tau_{3K} \rho_{30})(\partial^\mu - iq_{\bar{K}} A^\mu - ig_{\omega K} \omega_0 - ig_{\rho K} \tau_{3K} \rho_{30})\bar{K} + m_K^{*2} \bar{K} = 0, \quad (31)$$

and the energy spectra are obtained as

$$\omega_{K^-} = \sqrt{m_K^{*2} + k_z^2 + (2n+1)|q_{K^-}|B} - g_{\omega K} \omega_0 - g_{\rho K} \rho_{30}, \quad (32)$$

$$\omega_{\bar{K}^0} = \sqrt{m_K^{*2} + k_x^2 + k_y^2 + k_z^2} - g_{\omega K} \omega_0 + g_{\rho K} \rho_{30}. \quad (33)$$

For s -wave condensation of negatively charged K^- and neutral \bar{K}^0 , we have the chemical potentials

$$\begin{aligned} \mu_{K^-} &= \omega_{K^-} (n = k_z = 0) \\ &= \sqrt{m_K^{*2} + |q_{K^-}|B} - g_{\omega K} \omega_0 - g_{\rho K} \rho_{30}, \end{aligned} \quad (34)$$

$$\mu_{\bar{K}^0} = \omega_{\bar{K}^0} (k_x = k_y = k_z = 0) = m_K^* - g_{\omega K} \omega_0 + g_{\rho K} \rho_{30}. \quad (35)$$

The number densities of antikaons are given by

$$\rho_{K^-} = 2\sqrt{m_K^{*2} + |q_{K^-}|B} \bar{K} K, \quad (36)$$

$$\rho_{\bar{K}^0} = 2m_K^* \bar{K} K. \quad (37)$$

For neutron star matter with uniform distributions, the composition of matter is determined by the requirements of charge neutrality and β -equilibrium conditions. In the present calculation with antikaon condensation, the β -equilibrium conditions are expressed by

$$\mu_n - \mu_p = \mu_{K^-} = \mu_e = \mu_\mu, \quad (38)$$

$$\mu_{\bar{K}^0} = 0, \quad (39)$$

and the charge neutrality condition is given by

$$\rho_v^p = \rho_{K^-} + \rho_v^e + \rho_v^\mu, \quad (40)$$

with ρ_v^p and ρ_{K^-} given in Eqs. (23) and (36). The vector density of leptons has a similar expression to that of protons

$$\rho_v^l = \frac{|q_l| B}{2\pi^2} \sum_v \sum_s k_{f,v,s}^l. \quad (41)$$

We solve the coupled Eqs. (14)–(16) and (38)–(40) self-consistently at a given baryon density, $\rho_B = \rho_v^p + \rho_v^n$, in the presence of antikaon condensation and strong magnetic fields. The total energy density of neutron star matter is given by

$$\varepsilon = \varepsilon_p + \varepsilon_n + \varepsilon_{\bar{K}} + \varepsilon_l + \frac{1}{2} m_\sigma^2 \sigma^2 + \frac{1}{2} m_\omega^2 \omega_0^2 + \frac{1}{2} m_\rho^2 \rho_{30}^2, \quad (42)$$

where the energy densities of nucleons, antikaons, and leptons have the following forms:

$$\begin{aligned} \varepsilon_p &= \frac{q_p B}{4\pi^2} \sum_v \sum_s \left[k_{f,v,s}^p E_f^p + \left(\sqrt{M_N^{*2} + 2\nu q_p B} - s\kappa_p B \right)^2 \right. \\ &\quad \left. \times \ln \left| \frac{k_{f,v,s}^p + E_f^p}{\sqrt{M_N^{*2} + 2\nu q_p B} - s\kappa_p B} \right| \right], \end{aligned} \quad (43)$$

$$\begin{aligned} \varepsilon_n &= \frac{1}{4\pi^2} \sum_s \left\{ \frac{1}{2} k_{f,s}^n E_f^{n3} - \frac{2}{3} s\kappa_n B E_f^{n3} \right. \\ &\quad \times \left(\arcsin \frac{M_N^* - s\kappa_n B}{E_f^n} - \frac{\pi}{2} \right) \\ &\quad - \left(\frac{s\kappa_n B}{3} + \frac{M_N^* - s\kappa_n B}{4} \right) \\ &\quad \times \left[(M_N^* - s\kappa_n B) k_{f,s}^n E_f^n \right. \\ &\quad \left. + (M_N^* - s\kappa_n B)^3 \ln \left| \frac{k_{f,s}^n + E_f^n}{M_N^* - s\kappa_n B} \right| \right] \right\}, \end{aligned} \quad (44)$$

$$\varepsilon_{\bar{K}} = \sqrt{m_K^{*2} + |q_{K^-}|B} \rho_{K^-} + m_K^* \rho_{\bar{K}^0}, \quad (45)$$

$$\begin{aligned} \varepsilon_l &= \sum_{l=e,\mu} \sum_v \sum_s \frac{|q_l| B}{4\pi^2} \left[k_{f,v,s}^l E_f^l + (m_l^2 + 2\nu |q_l| B) \right. \\ &\quad \left. \times \ln \left| \frac{k_{f,v,s}^l + E_f^l}{\sqrt{m_l^2 + 2\nu |q_l| B}} \right| \right]. \end{aligned} \quad (46)$$

The antikaons do not contribute directly to the pressure because they are in the s -wave condensation. The pressure of the system can be obtained by

$$P = \sum_i \mu_i \rho_v^i - \varepsilon = \mu_n \rho_B - \varepsilon. \quad (47)$$

We note that the contribution from electromagnetic fields to the energy density and pressure, $\varepsilon_f = P_f = B^2/8\pi$, is not taken into account in the present calculation. In general, the strong magnetic fields in neutron stars can produce magnetic forces that play an important role in determining the structure of the star [4].

III. RESULTS AND DISCUSSION

In this section, we analyze the properties of neutron star matter with antikaon condensation in the presence of strong magnetic fields using the QMC model. The effective masses of nucleons and kaons in the QMC model are obtained self-consistently at the quark level, which is the main difference from the RMF model [30]. To show how the results depend on the models based on different degrees of freedom, we make a systematic comparison between the QMC model and the RMF model with the TM1 parameter set [31]. As a nonlinear version of the RMF model, the TM1 model has been widely used in many studies of nuclear physics [11,32–35]. The TM1

model includes nonlinear terms for both σ and ω mesons, and its parameters were determined by reproducing the properties of nuclear matter and finite nuclei including neutron-rich nuclei [31]. It has been pointed in Refs. [16,17] that antikaon condensation in the RMF models is quite sensitive to the antikaon optical potential at normal nuclear matter density, $U_{\bar{K}}(\rho_0) = g_{\sigma K}\sigma - g_{\omega K}\omega_0$. In the QMC model, the antikaon optical potential is given by $U_{\bar{K}} = m_K^* - m_K - g_{\omega K}\omega_0$ [22], and we obtain $U_{\bar{K}}(\rho_0) = -123$ MeV with the parameters used in the present study, which agrees with the result given in Ref. [22]. We note that the basic coupling constants in the QMC model are defined at the quark level. Therefore, $U_{\bar{K}}(\rho_0)$ is a predicted value with determined g_{σ}^q and g_{ω}^q . However, $U_{\bar{K}}(\rho_0)$ in the RMF model is usually taken to be in a range and used to determine the kaon-meson couplings. Here we take $g_{\omega K} = g_{\omega N}/3$ and $g_{\sigma K} = 0.926$ in the TM1 model, which is determined by fitting $U_{\bar{K}}(\rho_0) = -123$ MeV obtained in the QMC model, so the comparison between the QMC and TM1 models is more meaningful. It is well known that the direct URCA process produces the most powerful neutrino emission in the core of neutron star and leads to rapid cooling of the star. In the QMC model at $B = 0$, the direct URCA process occurs at the critical density $\rho_{\text{URCA}} \approx 0.29$ fm $^{-3}$, which implies the direct URCA process can take place for neutron star with gravitational mass $M > 1.08 M_{\odot}$. These values in the TM1 model are $\rho_{\text{URCA}} \approx 0.21$ fm $^{-3}$ and $M > 0.81 M_{\odot}$. We note that the maximum masses of neutron stars adopting the QMC and TM1 equations of state with antikaon condensation in the field-free case are about $1.85 M_{\odot}$ and $2.09 M_{\odot}$, respectively.

In this article, we present numerical results for the magnetic field strengths $B^* = B/B_c^e = 0, 10^5$, and 10^6 ($B_c^e = 4.414 \times 10^{13}$ G is the electron critical field). We note that the magnetic fields $B^* = 10^5$ and 10^6 may be too large for static configurations of neutron stars to exist. In Ref. [36], the authors performed relativistic calculations of axisymmetric neutron star. They found that the maximum allowable poloidal magnetic field is of the order of 10^{18} G when the magnetic pressure is comparable to the fluid pressure at the center of the star. In Ref. [4], the authors studied static neutron stars with poloidal magnetic fields and a simple class of electric current distributions, and they obtained that the maximum magnetic field strengths at the center of neutron stars could be as large as about 5×10^{18} G.

We show in Fig. 1 the effective masses of nucleons and kaons as a function of the baryon density in neutron star matter for $B^* = 0, 10^5$, and 10^6 . The results of the QMC model in the upper panel are compared with those of the TM1 model in the lower panel. It is shown that the effective nucleon masses in the QMC model are larger than those in the TM1 model, but the opposite is true for the effective kaon masses. Note that the effective masses of nucleons and kaons in the QMC model are obtained self-consistently at the quark level, whereas they are simple linear functions of σ in the TM1 model. We find that the influence of the magnetic field on the effective masses is not observable until $B^* > 10^5$, and the effective masses of both nucleons and kaons in strong magnetic fields are larger than the field-free values. In Fig. 2, we present the antikaon fractions, $Y_{K^-} = \rho_{K^-}/\rho_B$ (left panels) and $Y_{\bar{K}^0} = \rho_{\bar{K}^0}/\rho_B$ (right panels), again for $B^* = 0, 10^5$, and 10^6 . It is seen that the threshold

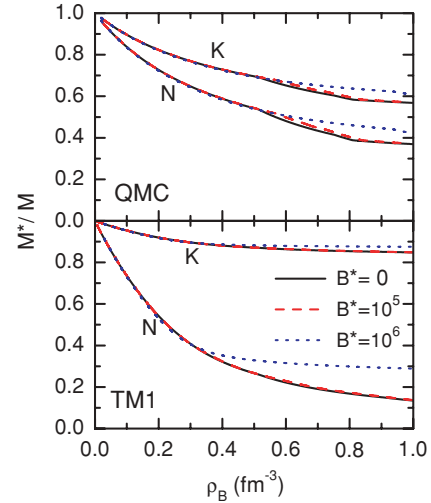


FIG. 1. (Color online) The effective masses of nucleons and kaons, M^*/M , as a function of the baryon density, ρ_B , for the magnetic field strengths $B^* = 0, 10^5$, and 10^6 . The results of the QMC model shown in the upper panel are compared with those of the TM1 model shown in the lower panel.

density of antikaon condensation is significantly changed by the magnetic field when B^* is large enough. In the QMC model (upper panels), the threshold densities of K^- condensation are 0.513, 0.572, and 1.277 fm $^{-3}$ corresponding to $B^* = 0, 10^5$, and 10^6 , whereas those of \bar{K}^0 condensation are 0.750, 0.728, and 0.934 fm $^{-3}$, respectively. In contrast, for the TM1 model in the lower panels, the threshold densities are 0.514, 0.588, and 1.732 fm $^{-3}$ for K^- condensation, whereas they are 0.905, 0.885, and 1.316 fm $^{-3}$ for \bar{K}^0 condensation. We note that the results of the TM1 model shown in Refs. [11,16] can be obtained using twice lower $g_{\rho N}$ than given in Ref. [31]. Therefore, they are different from our results of the TM1 model.

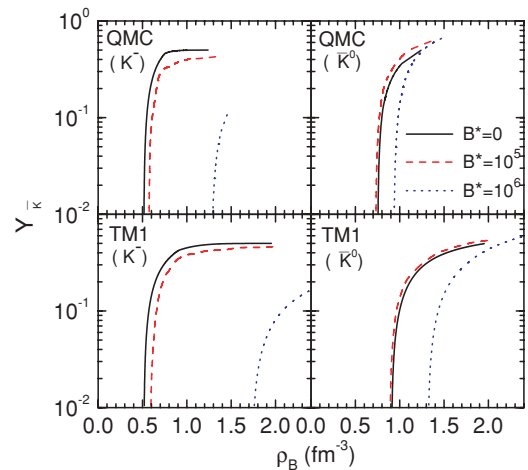


FIG. 2. (Color online) The antikaon fractions, Y_{K^-} (left panels) and $Y_{\bar{K}^0}$ (right panels), as a function of the baryon density, ρ_B , for $B^* = 0, 10^5$, and 10^6 . The results of the QMC and TM1 models are shown in the upper and lower panels, respectively.

It is very interesting to compare the effect of the magnetic field on K^- and \bar{K}^0 condensations. The onset of K^- condensation shifts to higher density in the presence of strong magnetic fields, and it even occurs beyond the threshold of \bar{K}^0 condensation. This is mainly because the negatively charged K^- gets a large chemical potential in the presence of strong magnetic fields, as given in Eq. (34) due to the term $|q_{K^-}|B$. However, the threshold density of \bar{K}^0 condensation for $B^* = 10^5$ is slightly smaller than the field-free value, whereas the one for $B^* = 10^6$ significantly increases. Although \bar{K}^0 is a neutral particle, its chemical potential given by Eq. (35) is indirectly influenced by the magnetic field through the dependence of meson mean fields on the magnetic field. We conclude that K^- condensation depends more on the magnetic field than does \bar{K}^0 condensation. By comparing the results of the QMC model with those of the TM1 model, one can see that the onset of antikaon condensation in the presence of strong magnetic fields occurs at lower densities within the QMC model. This is because the chemical potentials of antikaons in the QMC model decrease more rapidly than those in the TM1 model. We note that the threshold densities of antikaon condensation is mainly determined by the behavior of the chemical potentials, and the chemical potentials are related to the meson fields by Eqs. (34) and (35). Because the TM1 model includes nonlinear terms for both σ and ω mesons, the density dependence of the meson fields in the TM1 model is quite different from those in the QMC model, and it leads to different behavior of the chemical potentials in the two models. Although there are quantitative differences between the QMC and TM1 models, we find that qualitative trends of magnetic field effects are similar in the two models.

In Figs. 3, 4, and 5, we show the electron fraction $Y_e = \rho_e^e / \rho_B$, the muon fraction $Y_\mu = \rho_\mu^\mu / \rho_B$, and the proton fraction $Y_p = \rho_p^p / \rho_B$ as functions of ρ_B for $B^* = 0, 10^5,$

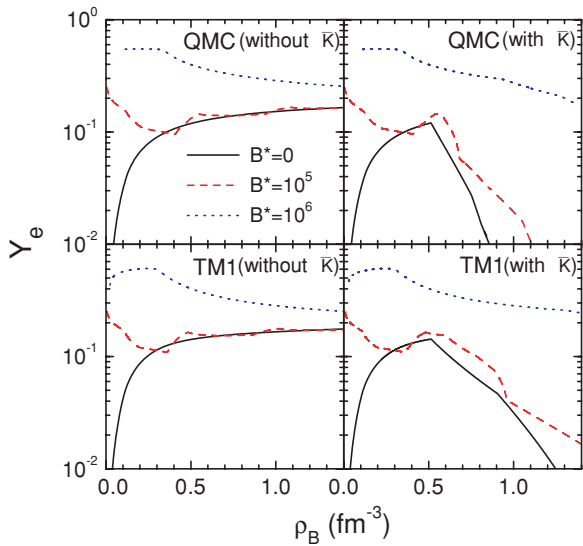


FIG. 3. (Color online) The electron fraction, Y_e , as a function of the baryon density, ρ_B , for $B^* = 0, 10^5,$ and 10^6 . The results with and without \bar{K} condensation are shown in the right and left panels, respectively. The results of the QMC model shown in the upper panels are compared with those of the TM1 model shown in the lower panels.

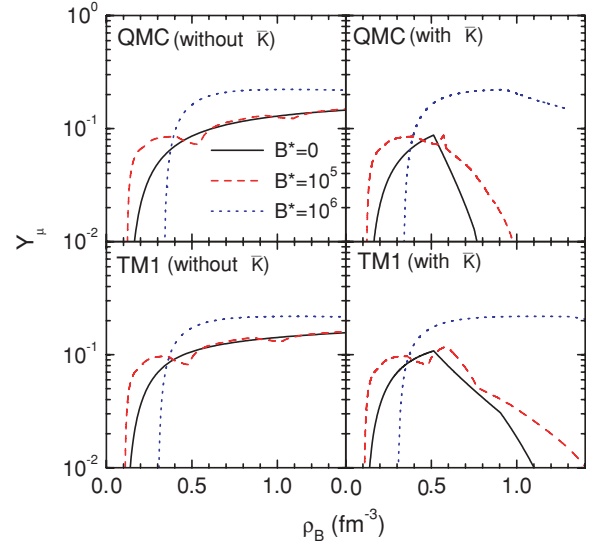


FIG. 4. (Color online) The muon fraction, Y_μ , as a function of the baryon density, ρ_B , for $B^* = 0, 10^5,$ and 10^6 . The results with and without \bar{K} condensation are shown in the right and left panels, respectively. The results of the QMC model shown in the upper panels are compared with those of the TM1 model shown in the lower panels.

and 10^6 . One can obtain the neutron fraction $Y_n = \rho_n^n / \rho_B$ as $Y_n = 1 - Y_p$. The charge neutrality condition gives the relation $Y_p = Y_{K^-} + Y_e + Y_\mu$. The results with and without \bar{K} condensation are displayed in the right and left panels, respectively. The negatively charged K^- play the same role as electrons and muons in maintaining the charge neutrality. Therefore, the presence of K^- condensation decreases Y_e and Y_μ as shown in the right panels of Figs. 3 and 4. In the presence of strong magnetic fields, the chemical potentials $\mu_e, \mu_\mu,$ and μ_{K^-} are influenced by the magnetic field. As a result, drops of Y_e and Y_μ in Figs. 3 and 4 become less steep for large magnetic field strength B^* . In Fig. 4, it is seen that the

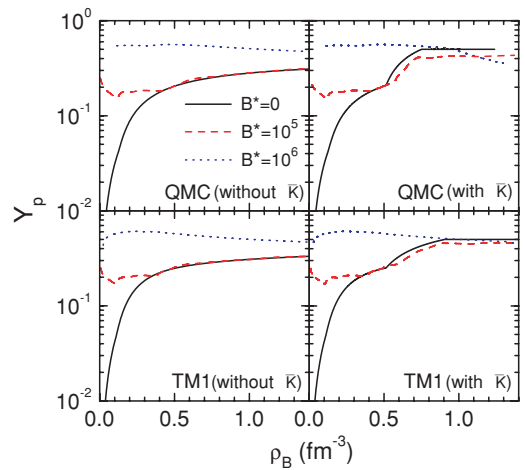


FIG. 5. (Color online) The proton fraction, Y_p , as a function of the baryon density, ρ_B , for $B^* = 0, 10^5,$ and 10^6 . The results with and without \bar{K} condensation are shown in the right and left panels, respectively. The results of the QMC model shown in the upper panels are compared with those of the TM1 model shown in the lower panels.

threshold densities for the appearance of muons are affected by the magnetic field. The threshold of muons for $B^* = 10^5$ is slightly smaller than the field-free value, whereas the one for $B^* = 10^6$ significantly increases. The presence of K^- condensation leads to an enhancement of Y_p as shown in the right panels of Fig. 5. At high density where \bar{K}^0 condensation occurs, $Y_p = 0.5$ is obtained for $B^* = 0$. This is because β -equilibrium conditions enforce $\rho_v^p = \rho_v^n$ as discussed in Ref. [16]. The feature is changed in the presence of strong magnetic fields, and we get $E_f^n - E_f^p = \sqrt{m_K^{*2} + |q_{K^-}|B} - m_K^*$ derived from the β -equilibrium conditions when the condensations of isospin doublet, K^- and \bar{K}^0 , occur together in neutron star matter. By comparing the right and left panels of Figs. 3, 4, and 5, we find that the presence of antikaon condensation can significantly change the particle fractions. It is obvious that the composition of neutron star matter with antikaon condensation depends on both the magnetic field strength B^* and the baryon density ρ_B . We note that the tendencies in the upper panels obtained in the QMC model are quite similar to those of the TM1 model in the lower panels of Figs. 3, 4, and 5. In the right panels of Figs. 3 and 4 where antikaons are included, Y_e and Y_μ decrease more rapidly at high densities in the QMC model than in the TM1 model. This is due to the same reason as that discussed for the earlier appearance of antikaon condensation in the QMC model. Because the β -equilibrium condition $\mu_{K^-} = \mu_e = \mu_\mu$ should be satisfied, μ_e and μ_μ in the QMC model decrease more rapidly than those in the TM1 model, just like the case of μ_{K^-} . This leads to a quicker drop in the upper right panels of Figs. 3 and 4 comparing with those in the lower right panels.

In Fig. 6, we show the matter pressure P as a function of the matter energy density ε for the magnetic field strengths $B^* = 0, 10^5$, and 10^6 . The results with and without \bar{K} condensation are plotted in the right and left panels, respectively. It is seen that the presence of \bar{K} condensation makes the EOS softer compared with the case without \bar{K} condensation. The softening of the EOS becomes less pronounced with increasing magnetic

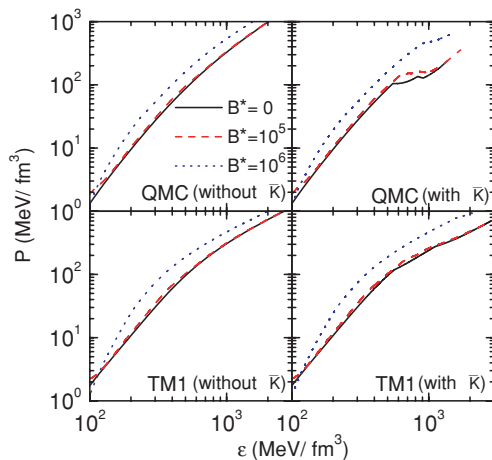


FIG. 6. (Color online) The matter pressure, P , versus the matter energy density, ε , for $B^* = 0, 10^5$, and 10^6 . The results of the QMC model with and without \bar{K} condensation are shown in the upper right and upper left panels, respectively. Those in the TM1 model are shown in the lower panels for comparison.

field for $B^* > 10^5$. This is because the threshold of antikaon condensation shifts to higher density and the effect of antikaon condensation on the EOS gets weaker with increasing B^* . At higher densities, the influence of strong magnetic fields on the EOS becomes noticeable as the field strength increases above $B^* \sim 10^5$. Here we include the anomalous magnetic moments of nucleons, which play an important role in the study of neutron star matter with strong magnetic fields as discussed in our previous work [8]. The results of the QMC model in the upper panels are compared with those of the TM1 model in the lower panels. The EOS in the QMC model is slightly softer than the one in the TM1 model.

IV. SUMMARY

In this article, we have studied the effects of strong magnetic fields on antikaon condensation in neutron star matter using the QMC model. Nucleons and antikaons in the QMC model are described as MIT bags that interact through the self-consistent exchange of scalar and vector mesons in the mean-field approximation. In the QMC model, the effective masses of nucleons and kaons are obtained self-consistently at the quark level, which is the main difference from the RMF models. It is clear that the effects of strong magnetic fields become significant only for magnetic field strength $B^* > 10^5$. We found that the presence of strong magnetic fields significantly alters the threshold density of antikaon condensation. The threshold of antikaon condensation shifts to higher density in the presence of strong magnetic fields. For $B^* = 0, 10^5$, and 10^6 , we obtained the threshold densities of K^- condensation are $0.513, 0.572$, and 1.277 fm^{-3} , whereas those of \bar{K}^0 condensation are $0.750, 0.728$, and 0.934 fm^{-3} . It is obvious that the threshold density of K^- condensation depends strongly on the magnetic field strength, and it even shifts beyond the threshold of \bar{K}^0 condensation for sufficiently strong magnetic fields. Because the negatively charged K^- can play the same role as electrons and muons in maintaining the charge neutrality, the presence of K^- condensation decreases the fractions of electrons and muons dramatically, and the drops become less steep for larger field strength. It is found that the presence of antikaon condensation can significantly change the composition of neutron star matter, and the particle populations depend on both the magnetic field strength B^* and the baryon density ρ_B .

The presence of antikaon condensation can make the EOS softer compared with the case without antikaon condensation. The softening of the EOS becomes less pronounced with increasing magnetic field for $B^* > 10^5$. It is known that the Landau quantization of charged particles causes a softening in the EOS, whereas the inclusion of nucleon anomalous magnetic moments leads to a stiffening of the EOS. At high densities, the softening of the EOS from Landau quantization with increasing magnetic field for $B^* > 10^5$ can be overwhelmed by the stiffening resulting from the incorporation of anomalous magnetic moments. We have made a systematic comparison between the results of the QMC and TM1 models. It is found that quantitative differences exist between the two

models, but qualitative trends of magnetic field effects on antikaon condensation and EOS are quite similar.

Finally, we would like to give a few remarks on the limitations of the results presented in this article. Although the QMC model is constructed at the quark level, it is certainly approximate due to several reasons. The MIT bag model itself is known to be a simplification, and the mean-field treatment for meson fields is an approximation. The adopted model of spherical bags can be violated in a superstrong magnetic field, because the magnetic localization length for protons on the ground Landau level with $B^* \sim 10^6$ is of the same order as the bag radius used in the present calculation. These approximations need to be examined more carefully in further

work. For neutron star matter at high density, hyperons may appear before the onset of antikaon condensation. It would be interesting and important to include hyperons and antikaon condensation in the study of neutron star matter with strong magnetic fields.

ACKNOWLEDGMENTS

This work was supported in part by the National Natural Science Foundation of China (no. 10675064) and the Specialized Research Fund for the Doctoral Program of Higher Education (no. 20040055010).

-
- [1] A. K. Harding and D. Lai, Rep. Prog. Phys. **69**, 2631 (2006).
 - [2] C. Thompson and R. C. Duncan, Astrophys. J. **473**, 322 (1996).
 - [3] A. Broderick, M. Prakash, and J. M. Lattimer, Astrophys. J. **537**, 351 (2000).
 - [4] C. Y. Cardall, M. Prakash, and J. M. Lattimer, Astrophys. J. **554**, 322 (2001).
 - [5] G. J. Mao, A. Iwamoto, and Z. X. Li, Chin. J. Astron. Astrophys. **3**, 359 (2003).
 - [6] S. Chakrabarty, D. Bandyopadhyay, and S. Pal, Phys. Rev. Lett. **78**, 2898 (1997).
 - [7] F. X. Wei, G. J. Mao, C. M. Ko, L. S. Kisslinger, H. Stocker, and W. Greiner, J. Phys. G **32**, 47 (2006).
 - [8] P. Yue and H. Shen, Phys. Rev. C **74**, 045807 (2006).
 - [9] A. Broderick, M. Prakash, and J. M. Lattimer, Phys. Lett. **B531**, 167 (2002).
 - [10] I.-S. Suh and G. J. Mathews, Astrophys. J. **546**, 1126 (2001).
 - [11] P. Dey, A. Bhattacharyya, and D. Bandyopadhyay, J. Phys. G **28**, 2179 (2002).
 - [12] H. Heiselberg and M. Hjorth-Jensen, Phys. Rep. **328**, 237 (2000).
 - [13] J. Schaffner and I. N. Mishustin, Phys. Rev. C **53**, 1416 (1996).
 - [14] S. Pal, M. Hanauske, I. Zakout, H. Stocker, and W. Greiner, Phys. Rev. C **60**, 015802 (1999).
 - [15] P. K. Panda, D. P. Menezes, and C. Providencia, Phys. Rev. C **69**, 025207 (2004).
 - [16] S. Pal, D. Bandyopadhyay, and W. Greiner, Nucl. Phys. **A674**, 553 (2000).
 - [17] S. Banik and D. Bandyopadhyay, Phys. Rev. C **63**, 035802 (2001); **64**, 055805 (2001); **66**, 065801 (2002).
 - [18] N. K. Glendenning and J. Schaffner-Bielich, Phys. Rev. Lett. **81**, 4564 (1998); Phys. Rev. C **60**, 025803 (1999).
 - [19] R. Knorren, M. Prakash, and P. J. Ellis, Phys. Rev. C **52**, 3470 (1995).
 - [20] J. A. Pons, S. Reddy, P. J. Ellis, M. Prakash, and J. M. Lattimer, Phys. Rev. C **62**, 035803 (2000).
 - [21] H. Guo, B. Liu, and J. W. Zhang, Phys. Rev. C **67**, 024902 (2003).
 - [22] D. P. Menezes, P. K. Panda, and C. Providencia, Phys. Rev. C **72**, 035802 (2005).
 - [23] P. Guichon, Phys. Lett. **B200**, 235 (1988).
 - [24] K. Saito, K. Tsushima, and A. W. Thomas, Nucl. Phys. **A609**, 339 (1996).
 - [25] H. Muller and B. K. Jennings, Nucl. Phys. **A640**, 55 (1998).
 - [26] K. Tsushima, K. Saito, J. Haidenbauer, and A. W. Thomas, Nucl. Phys. **A630**, 691 (1998).
 - [27] K. Saito, K. Tsushima, and A. W. Thomas, Prog. Part. Nucl. Phys. **58**, 1 (2007).
 - [28] K. Tsushima, K. Saito, A. W. Thomas, and S. V. Wright, Phys. Lett. **B429**, 239 (1998).
 - [29] D. B. Kaplan and A. E. Nelson, Phys. Lett. **B175**, 57 (1986).
 - [30] B. D. Serot and J. D. Walecka, Adv. Nucl. Phys. **16**, 1 (1986).
 - [31] Y. Sugahara and H. Toki, Nucl. Phys. **A579**, 557 (1994).
 - [32] H. Shen, H. Toki, K. Oyamatsu, and K. Sumiyoshi, Nucl. Phys. **A637**, 435 (1998).
 - [33] D. Hirata, K. Sumiyoshi, B. V. Carlson, H. Toki, and I. Tanihata, Nucl. Phys. **A609**, 131 (1996).
 - [34] H. Shen, Phys. Rev. C **65**, 035802 (2002).
 - [35] H. Shen, Y. Fang, and H. Toki, Prog. Theor. Phys. **115**, 325 (2006).
 - [36] M. Bocquet, S. Bonazzola, E. Gourgoulhon, and J. Novak, Astron. Astrophys. **301**, 757 (1995).